JOURNAL OF OPTOELECTRONICS AND ADVANCED MATERIALS, Vol. 10, No. 9, September 2008, p. 2396 – 2401

Effect of nitrogen addition on morphology and magnetic properties of electrodeposited Co-Ni granular films

C. SÎRBU, V. GEORGESCU
Faculty of Physics, "Alexandru Ioan Cuza" University, Iasi, 700506, Romania

The granular films of magnetic alloys consisting of nanoscale ferromagnetic particles which exhibit a giant magnetoresistance (GMR) effect have been a subject of great interest in recent years. In this work, we report on experimental investigation of the influence of nitrogen addition on magnetic and transport properties of Co–Ni granular films with different nitrogen content, and on the surface morphology. The correlation between these properties and the electrodeposition conditions has been studied. The granular thin films were electrodeposited onto a disk-shaped aluminium substrate, from a basic bath containing: $CoSO_4.7\ H_2O$, $NiSO_4.7\ H_2O$, and $NiCl_2.6H_2O$ with 20 gl^{-1} total metallic ion content. As additional substances were used NaCl, $Na_2SO_4.10\ H_2O$, H_3BO_3, sodium citrate, sodium laurylsulphate, sodium saccharine and $NaNO_3$ as a source for nitrogen inclusion in the films. The concentration of $NaNO_3$ in electrolytic bath was varied with the aim to control the films nitrogen content. Co-Ni-N granular films display GMR effect of about 60%; this could be explained mainly by the elastic spin dependent scattering of conduction electrons at the interface between magnetic (Co-Ni solid solution grains) and nonmagnetic regions (rich in N inter-granular frontiers and aluminium oxidized substrate).

(Received July 31, 2008; accepted August 14, 2008)

Keywords: Magnetic properties, Giant magnetoresistance, Thin films, Co-Ni Alloys, Electrodeposition

1. Introduction

Many studies have been carried out to develop ternary alloys based on Co-Ni system with additions, because of their remarkable magnetic properties and potential applications in high density recording [1, 2] or micro-electromechanical systems [3-7]. In recent years there have been a number of investigations on giant magneto-resistive granular films consisting of nano-scale ferromagnetic particles embedded in an immiscible non-ferromagnetic matrix [8-11]. The granular films with GMR effect have been studied due to simpler preparation than multilayer films and applications in information technology. It is known that the GMR effect in granular films originates from the spin-dependent scattering of conduction electrons at the interfaces between the ferromagnetic granules and the nonmagnetic matrix (metals or insulator) as well as within the ferromagnetic granules, and it has a close relationship with grain size.

Our goal was to obtain by electrodeposition granular films presenting GMR effect. Electrodeposited thin films of Co-Ni alloys with additions of magnesium and nitrogen studied in our previous works [12, 13] could be a potential candidate for such applications. Electrodeposition has many advantages over vacuum processes: especially extended surfaces at low costs, low operating temperatures and the possibility of large scale applications.

In this work, we propose a new method for obtaining Co-Ni granular films, namely by introducing nitrogen as impurity in the electrodeposited film. We report here on the experimental investigation of the influence of nitrogen addition on magnetic properties of Co–Ni granular films with different nitrogen content, and on the surface morphology. The correlation between these properties and the preparation conditions could be useful for technological applications. There are publications dealing with the magnetoresistance of electroplated Co-Ag granular films [10, 11], but we have not found in the literature any study referring to magnetic and transport properties in the case of electrodeposited Co-Ni granular films with addition of nitrogen.

2. Experimental

The samples were prepared by an electrolytic procedure similar with that used for producing Co-Ni-Mg-N thin films described in detail elsewhere [12, 13]. A complex bath was used, containing: $CoSO_4.7\ H_2O$, $NiSO_4.7\ H_2O$, and $NiCl_2.6H_2O$ with 20 gl^{-1} total metallic ion content, and the additional substances: NaCl, $Na_2SO_4.10H_2O$, H_3BO_3, sodium citrate, sodium laurylsulphate, and sodium saccharine. The deposition performed from this base electrolytic bath (labelled 1) leads to Co-Ni films. If the bath contains $NaNO_3$ as addition, the deposited Co-Ni films will contain nitrogen as impurity. It was shown [12, 13] that the concentration (c) of $NaNO_3$ in electrolytic bath controls the nitrogen content (C_N) of the film. The film thickness for all the samples was controlled by the current density and the deposition time.

Cyclic voltammetry was mainly employed as the electrochemical technique for the study of electrodeposition processes.

The quantitative chemical composition of the films was determined by EDAX. The surface analyses were

performed with an atomic force microscope (AFM) at room temperature in tapping mode, using a commercial Si_3N_4 tip with a radius of 10 nm. The structure of the samples was investigated by X-ray diffraction using CoK_α radiation in the usual θ–2θ geometry.

The magnetic measurements were carried out at room temperature with a torsion magnetometer in 300 kA/m maximum field. Magnetoresistance (MR) measurements at room temperature were carried out with an HM 8112-2 programmable multimeter, by usual 2-terminals method in dc magnetic field between −300 and +300 kA/m, applied perpendicular to the current, in plane of the film. MR was measured at constant current of 7 μA. Magnetoresistance was defined as

$MR = \frac{R_0 - R_S}{R_S} \times 100\%$, where R_0 denote the resistance measured in demagnetized state of the film and R_s denote the resistance in the maximum applied magnetic field.

3. Results and discussion

With the aim to characterize the electrodeposition process, the measurements of cyclic voltammograms were carried out in the electrolytic cell with the working electrode of Al and the anode of Ni as vertically placed disk-shaped foils. The geometrical area of an electrode was 3.14 cm^2. The reference electrode was a platinum wire having with the electrochemical solution the contact area of 0.06 mm^2.

As example, we present in figure 1 the voltammograms recorded for three solutions containing the base components of the bath 1 and various content *c* of $NaNO_3$. The density of current *versus* potential (between cathode and reference electrode) curves for the three solutions are shown in figure 1(a, b, and c), as follows: a) solution 1 with *c*=0, b) solution 2 with *c*=0.33g/l, and c) solution 3 with *c*=1.33g/l. The curves plotted at the increasing negative electrode potential (at the rate 2 mV/s) are marked with F (forward) and those plotted at the decreasing one, with B (backward).

The voltammograms in figure 1 shows typical characteristics of the electrodeposition of metal ions under the nucleation and crystal growth control: virtually zero current on the forward scan until the onset of the nucleation of Ni and Co ions and a rapid increase of current on the forward scan once the nucleation begins. The rapid increase of the cathodic current on the forward scan corresponds to the beginning of the metal deposition. The onset potential for the Co nucleation is increased to about –1.1V and for Ni it is of about -1.18V (*versus* Pt reference electrode) in our base solution, which are of a bigger value than that for the electrodeposition in equilibrium conditions for Ni and Co ions (-1.43V for Ni^{2+} and -1.48V for Co^{2+}, calculated *versus* Pt). The shape of the reversal scan B is completely different from that of the forward scan F (figure 1a). The onset potential on curve B was observed at -0.38V, which could be explained by the fact that the cathode surface at the beginning of the forward scan was Al substrate, and the cathode surface at the end of the reverse scan is covered with Co-Ni alloy. Also, the forward scan has a shape indicating the dissipative irreversible processes occurring at potentials between -1.35V and -1.6V. Therefore, it can be concluded that the electrochemical processes on the forward and reverse scans occur in an irreversible manner in the solution 1.

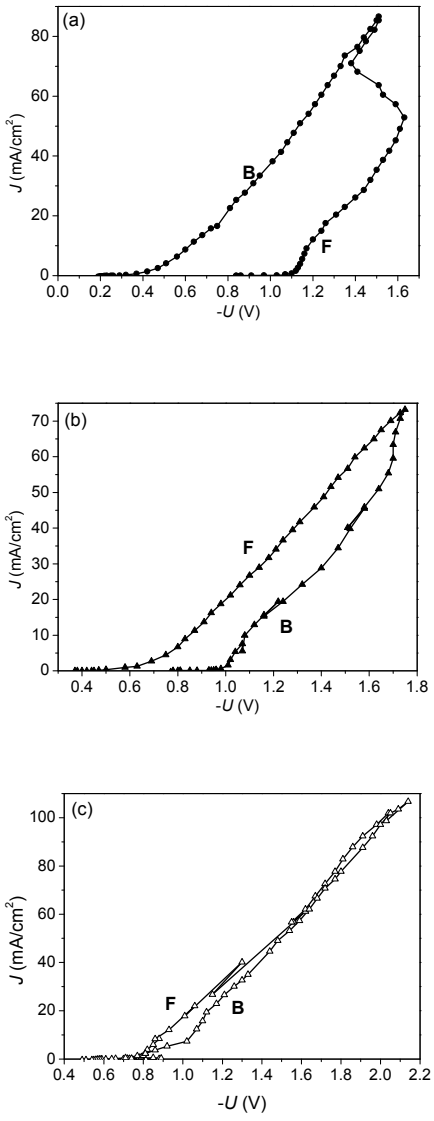

Fig.1 Current-voltage curves for three solutions with different concentration of $NaNO_3$: a) 0, b) 0.33 g/l and c) 1.33 g/l.

When the $NaNO_3$ is added in the base solution, the F and B scans draw nearer (figures 1b, 1c) which signify more reversible paths. The onset potential for the Co and Ni nucleation in the case of solution 2 (scan F) are -0.98V, -1.02V, respectively, and for the solution 3 they are: -0.78V, -1.01V, respectively. For the reverse scans, the onset potentials are: -0.47V (for the case of solution 2) and -0.71V (for solution 3). The irreversibility of the F and B current-voltage curves from fig. 1(a) indicates that the processes occurring in this case are irreversible; in the case

of the solution 3 (fig. 1c) the paths F and B are almost similar (showing nearly reversible processes). As we have found from the XRD and AFM measurements, which will be presented in the following section, the electrochemical plating regime influences the structure and morphology of the samples.

With the three solutions (1, 2, 3) we deposited in potentiostatic regime (at -1.5V *versus* Pt reference electrode) a series of samples (labelled I, II, III, respectively) with average thickness of 400 nm. The films were electrodeposited onto a disk-shaped aluminium substrate.

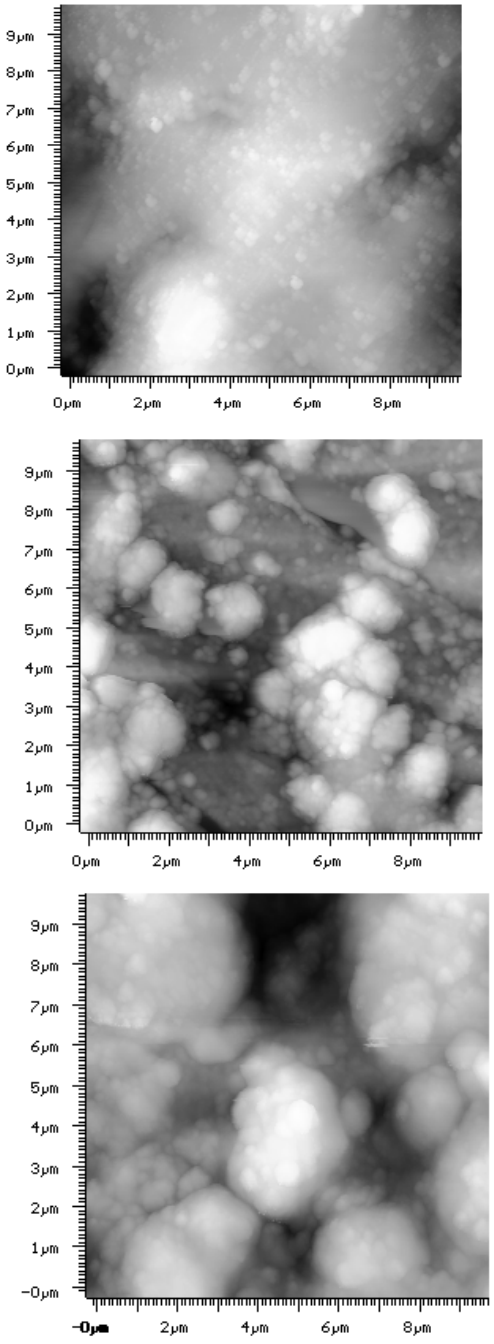

Fig.2. The topographic AFM images for the samples deposited in solutions with different $NaNO_3$ content: a) 0, b) 0.33 g/l and c) 1.33 g/l.

The surface morphology of the electrodeposited films (shape and size of crystallites) changes as a result of the different content of $NaNO_3$ in solution. Fig.2 shows the AFM topographic images for three typical samples: I (figure 2a), II (figure 2b) and III (figure 2c). The AFM images prove a three-dimensional progressive nucleation and crystal growth mechanism for the electrodeposition of the Co-Ni alloy. We suppose that the nitrogen atoms were chemisorbed on the cathode surface especially on the sites of newly formed nuclei. This could be partially responsible for the unchanged value for forward-backward directions of the onset nucleation potential as observed in the voltammetry experiments (figure 1c).

We can explain the inclusion of nitrogen in Co-Ni electrodeposited films by a similar process with that used for the removal of nitrate from brine wastes by electro catalytic conversion of nitrate to nitrogen [14]. The electrochemical reduction of NO_3^- in 0.1 M K_2SO_4 and 0.05 M KNO_3 solution was studied on various electrodes [15]. The products in all cases have been NO_2^-, NH_3, N_2 and small amounts of *NO*; aluminium was considered one of the more efficient cathodes as regards the conversion of NO_3^- to N_2. The mechanism of the nitrate reduction is complicated, because of its multi-electron nature and the presence of a large number of intermediates. The experiments from [15] were performed at very negative potentials, where the nitrate ions are strongly repelled by the likely charged electrode surface, so the observed increase in the rate of the reduction with the increase of the negative potential was unexpected. The authors give an explanation for this phenomenon by the theory of cationic catalysis [16]. According to this theory, the non–reacting cation of the supporting electrolyte in the interfacial region, acts as an attracting centre for the NO_3^- by forming virtual ion pairs of the type $Na^{\cdots}NO_3$ which can not be repelled by the negatively charged electrode [14, 15]. We suppose that the mechanism of cationic catalysis could be responsible for inclusion of N in Co-Ni films electrodeposited in our baths.

As it can be seen in figure 2, the addition of $NaNO_3$ exhibits a strong influence on the morphology of the film. The surface morphology (shape and size of the crystallites) is different in the three typical samples. For c = 0, the formation of a compact thin Co-Ni thin film is observed (figure 1a). By addition of $NaNO_3$ in the electrolytic bath, the deposits became granular and the aluminium substrate remains partially uncovered. From AFM topographic images one can conclude that small spherical nuclei nucleate in different sites on the substrate and sometimes they agglomerate (figure 2b). The analysis of the distribution of elements in these images by EDAX experiments are in progress. Preliminary results prove that Al and O are present in the un-deposited sites of the surface, for the samples II and III. For c = 1.33 g/l, the creation of aggregates of crystallites is enhanced, with some uncovered sites (holes) between aggregates (figure

2c). We suppose that the sample I, containing 81.20 at. % Co, 18.80 at.% Ni (with no evidence of Al, N, or O) is a compact Co-Ni thin film. For the sample II, if we consider the aggregates constituted especially from Co-Ni solid solution (76.95 at. % Co, 23.05 at. % Ni), the remaining surface between granules contains N, Al, and O. For the sample III, there is the same evidence for aggregates from Co-Ni solid solution (79.78 at. % Co, 20.21 at. % Ni), the remaining surface between granules contains N, Al, and O.

The electrolysis parameters have been the same for the deposition of the three representative samples (-1.5V, 30°C, without stirring), and the charge passing through electrolytic cell was also the same, resulting in the formation of a continuum film of 400 nm thickness (sample I) and equivalent average thickness for the granular samples (II and III).

A significant change in morphology (figures 2b, c) appears as a result of including $NaNO_3$ as additive in the electrolytic bath. The mean square roughness of the three samples (calculated from the 10 μm × 10 μm AFM topography scan) has the following values: (I) 45.70 nm, (II) 148.31 nm and (III) 182.34 nm. At the same time, the crystallite sizes with globular shapes are different in these samples. It is evident an agglomeration of crystallites (aggregates) when the additive content increases. The nitrogen adsorbed at the cathode surface creates disorder in the incorporation of ad-atoms into the lattice or inhibits the surface diffusion of ad-atoms towards growing centres. This is an evidence of the inhomogeneous growth of the crystallites on different nucleation sites. In other words, the film nucleation and growth process is modified as an effect of $NaNO_3$ as additive in the electroplating solution, with a preference for the N or NO ions to be adsorbed on the edge of grains, and thus gives rise to a globular structure and aggregates.

The XRD analyses indicated that our samples are constituted from a Co-Ni solid solution with a polycrystalline fcc lattice for the samples II and III, and it appears as amorphous for the sample I. For the samples II and III, the peaks from Al substrate appear also in XRD patterns, which confirm the existence of un-deposited sites on the Al surface, in a good concordance with AFM images (figures 2b and 2c). From correlation between AFM, EDX and XRD preliminary measurements we can conclude that magnetic granular films consisting of nano-scale Co-Ni ferromagnetic particles and aggregates are set in an immiscible non-ferromagnetic matrix (rich in aluminium and nitrogen addition). The morphology investigations are also supported by the magnetic measurements, as we will present shortly in the following results.

The shape of curve obtained by torsion magnetometer is a very sensitive function of the sample magnetic microstructure. Figure 3 shows as an example the torsion magnetometer curves of the sample III deposited in the solution 3, containing c=1.33g/l $NaNO_3$. The film plane was oriented perpendicular to the field-rotation plane; e. g. the torque was measured around an arbitrary axis parallel to the film plane. The torque curves were initiated with the applied field in the plane of the sample. The curves plotted in figure 3 were labeled with F (forward) and B (backward) for the rotation in clockwise direction and in the reversed one, respectively. In the torque experiment a magnetic field

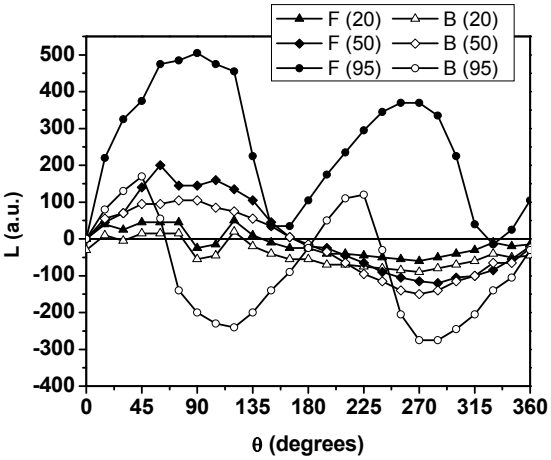

Fig.3. Torque curves for the sample III, plotted from 0 to 360 degrees (F) and from 360 to 0 degrees (B). The torque curves were measured for the fields: 20 kA/m, 50kA/m and 95 kA/m (marked in the legend).

is rotated from the film plane ($\theta = 0$ to the normal of the film, $\theta = \pi/2$) and the magnetization M follows at an angle φ with respect to the film plane. An equilibrium orientation for the magnetization is reached when the torques (L) on M due to H and to the total uniaxial anisotropy K_{eff} cancel. This could be described by $MHV\sin(\theta-\varphi) = L = K_{eff}\sin(2\varphi)$, where V is the magnetic volume of the film. At high fields, the magnetization is saturated ($\theta = \varphi$), and K_{eff} can be determined directly using this equation.

Granular Co-Ni-N films have unidirectional anisotropy evidenced by the sin θ shape of the torque curve in low fields and the increase of hysteresis loss in high magnetic field (figure 3); the presence of antiferromagnetic coupling between magnetic moments, due to inter-granular limits containing more N than the crystallites core results in this type of magnetic behaviour. As it can be seen in figure 3, the experimental torque curves exhibit mainly a two-fold periodicity in high fields. In low fields, a four-fold periodicity (i. e. the presence of an anisotropy energy term $K_2.\sin(4\varphi)$ can be observed for curves F and B measured in fields of 20kA/m and 50 kA/m. This four-fold periodicity can be explained by the simultaneous existence of regions with positive and negative K_{eff}, therefore by heterogeneity of magneto-crystalline anisotropy term in different aggregates. The curves in figure 3 indicate that the easy axis of magnetization for this sample is out of plane. The most probable source of out of plane anisotropy could be the columnar shape of the particles and aggregates.

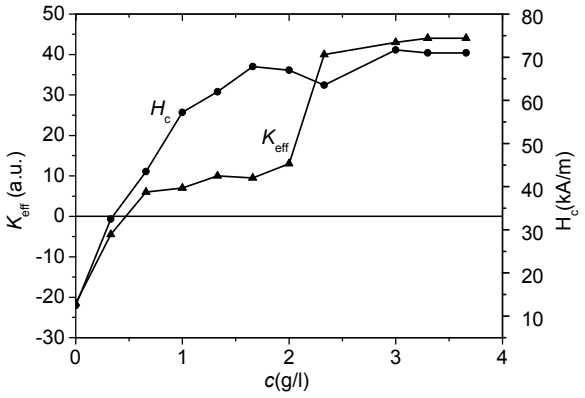

Fig. 4. The dependence of coercive field (H_c) and of effective anisotropy constant (K_{eff}) of electrodeposited granular Co-Ni films on the $NaNO_3$ content of the solution.

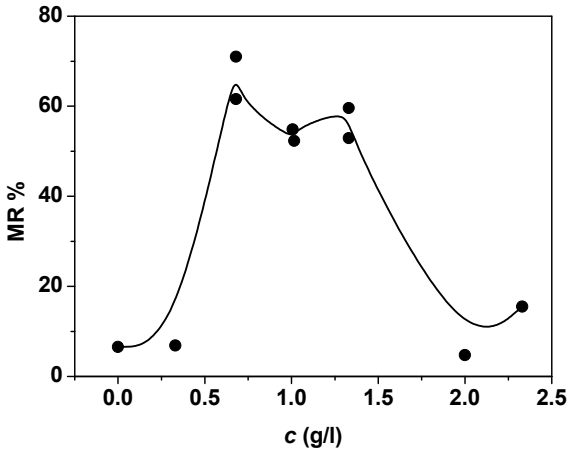

Fig.5. Magnetoresistance of some samples deposited from solutions with different c, at room temperature (line is only a guide for the eyes).

The dependence of the magnetic properties of the films (i.e. coercive field H_c, magnetic anisotropy constant K_{eff}) was also studied as a function of the $NaNO_3$ concentration in solution (figure 4). The values of these characteristics varied in the range H_c = (5 - 70) kA/m and K_{eff} = -20*10^4 J/m^3 to +40*10^4 J/m^3 depending on *c*.

From these measurements, we have found that magnetic behaviour of Co-Ni films is: a) ferromagnetic with easy plane of magnetization, for the films prepared in solution without $NaNO_3$ addition and b) ferromagnetic with out of plane easy axis, for those prepared in solution with addition. The dependence on *c* of magnetic behaviour of these films could be explained by changes in phase content and granular morphology of the samples by nitrogen addition.

The magnetoresistance ratio increases firstly with the N concentration and reaches a maximum for *c* = (0.66 – 1.35) g/l and then drops slowly. We can find very large values (around 60%) for GMR of the granular films deposited in these conditions.

Giant magnetoresistance in such granular films could be explained mainly by the elastic spin dependent scattering of conduction electrons at the interface between magnetic (Co-Ni solid solution grains) and nonmagnetic regions (aluminium oxidized substrate islands and rich in nitrogen inter-granular regions). The applied field changes the magnetic configuration of the system, which also depends on the temperature and the grain size distribution of the magnetic particles. The magnetic heterogeneity of such granular samples may increase the GMR effect, as it was observed in granular Co-Ag films [17]. It was shown theoretically [17], that the spin-dependent scattering on paramagnetic impurities and/or small paramagnetic clusters in the nonmagnetic metal is strongly enhanced in heterogeneous magnetic systems as compared to nonmagnetic metals with dissolved magnetic impurities.

The enhancement is due to the difference in the resistance of the spin-up and spin-down conduction channel, which does not cancel out if the spin diffusion length is sufficiently large. We have found that the GMR effect is very sensitive to the granular structure controlled by nitrogen addition, as well as to the specific magnetic interactions among the grains separated by thin insulating barriers (containing more nitrogen than the grains) because it involves the spin-dependent scattering of the conduction electrons by the magnetic impurities.

4. Conclusions

Co-Ni granular films containing N as additions were electrodeposited on aluminium substrates using a complex solution containing $NaNO_3$, in order to modify the film morphology and the magnetic and transport properties of the films.

The adsorption of nitrogen on the electrolyte/film interface by a cation catalysis effect results in morphology changes in granular films. The magnetic characteristics and the morphology of the electrodeposited Co-Ni films were found to strongly depend on the additive concentration of the electrolytic bath. The easy axis of magnetization is oriented out of plane for the samples deposited from solution with $NaNO_3$ addition. The magnetic properties are very sensitive to the grain structure, controlled by nitrogen addition and to the specific magnetic interactions among the grains. The grains are separated by thin insulating interfaces which are richer in N than the grain cores and aluminium oxidized islands from substrate.

We have found a correlation between the current-voltage curves recorded in solutions with different concentration of $NaNO_3$ and the results from X-ray analysis: namely, the irreversibility/reversibility from current-voltage curves could be correlated with structure

features, amorphous/ crystalline, respectively.

The Co-Ni-N granular films electrodeposited in solutions with c = (0.66 – 1.35) g/l display a large GMR effect (60%); they could be useful for applications in electronics. It is both easy and economical to produce by electrolysis Co–Ni-N granular films. The method needs no vacuum and can be easily mastered. So, it has a good perspective in the prospective industrial production, especially, is suited to produce low-cost magnetic sensors.

References

[1] Y. Nakamura, J. Magn. Magn. Mater., **200,** 634 (1999).
[2] T. Homma, Y. Kita, T. Osaka, J. Electrochem. Soc., **147**(1), 160 (2000).
[3] T.-S. Chin, J. Magn. Magn. Mater., **209,** 75 (2000).
[4] J.W. Judy, R.S. Muller, J. Microelectromechanical Sys., **6** (3), 249 (1997).
[5] J.W. Judy, R.S. Muller, H.H. Zappe, J. Microelectromechanical Sys., **4** (4), 162 (1995).
[6] T. Homma, Y. Sezai, T. Osaka, Y. Maeda, D.M. Donnet, J. Magn. Magn. Mater., **173** 314 (1997).
[7] N.V. Myung, D. Y. Park, B. Y. Yoo, P. T. A. Sumodjo, J. Magn. Magn. Mater., **265,** 189 (2003).
[8] J.Q. Xiao, J.S. Jiang, C.L. Chien, Phys. Rev. Lett. **68,** 3749 (1992).
[9] A.E. Berkowitz, J.R. Mitekell, M.J. Corey, et al., Phys.Rev. Lett., **68,** 3745 (1992).
[10] Ch. Wang, Zh. Guo, Y. Rong, T. Y. Hsu, J. Magn. Magn. Mater., **277,** 273 (2004).
[11] T. Y. Chen, S. X. Huang, C. L. Chien and M. D. Stiles, Phys. Rev. Lett., **96** (20), 207203 (2006).
[12] V. Georgescu, Mat. Sci. Eng., B**27,** 17 (1994).
[13] Violeta Georgescu, Mihaela Georgescu, J. Magn. Magn. Mater., **242-245,** 416 (2002).
[14] Polatides, C., Kyriacou, G., J. Appl. Electrochem. **35,** 421 (2005).
[15] I. Katsounaros, D. Ipsakis, C. Polatides, G. Kyriacou, Electrochimica Acta, **52,** 1329 (2006).
[16] Kotov, V.Yu, Tsirlina, G.A., Russ. Chem. Bull. **52,** 2393 (2003).
[17] A. Milner, I. Ya. Korenblit, and A. Gerber, Phys. Rev. B **60**, 14821 (1999).

*Corresponding author: cristina.sirbu@uaic.ro